JCTC Journal of Chemical Theory and Computation

Ab Initio and DFT Conformational Studies of Propanal, 2-Butanone, and Analogous Imines and Enamines

Haizhen Zhong,[†] Eugene L. Stewart,[‡] Maria Kontoyianni,[§] and J. Phillip Bowen*[,†]

Center for Drug Design, Department of Chemistry and Biochemistry, University of North Carolina at Greensboro, Greensboro, North Carolina 27402, Computational Center for Molecular Structure and Design, Department of Chemistry, University of Georgia, Athens, Georgia 30602, and Laboratory for Molecular Modeling, Division of Medicinal Chemistry and Natural Products, School of Pharmacy, University of North Carolina at Chapel Hill, Chapel Hill, North Carolina 27599

Received November 11, 2004

Abstract: The potential energy surfaces (PES) of 2-butanone, 2-butanimine, 1-butenamine, propanal, and propanimine have been explored with ab initio and DFT calculations at the RHF/6-311G**, MP2/6-311G**, and B3LYP/6-311G** levels of theory. In agreement with previous experimental and computational results, the PES provides two minima for each of the above molecules with the exception of 2-butanone, which clearly shows three distinct minima. Factors influencing the conformational preferences are also elaborated. Our calculations suggest that for 2-butanone and propanal, the steric and the bond dipole interactions are primarily responsible for the conformational preferences of these compounds. Additional charge−charge interactions might also play an important role in determining the imine conformations. For enamines, however, steric interactions play a critical role, with bond dipole interactions exerting some influence. Our results also suggest that for imine formation from butanone and/or propanal, the imine is the predominant product, not the enamine, which is consistent with experimental observations. Therefore, these calculations should provide a better understanding of the ketone/aldehyde to imine and enamine transformations. This transformation may introduce an important imine moiety for the analogues of *trans-N*-methyl-4-(1-naphthylvinyl)pyridine (NVP), a choline acetyltransferase (ChAT) inhibitor.

Introduction

Imine formation is a particularly important chemical reaction in many biological processes.[1,2] For example, the covalent binding of carbonyl-containing compounds to an enzyme usually involves the formation of an imine. The imine moiety is formed by condensation of a ketone (or aldehyde) carbonyl group with a primary or secondary amine. Equilibrium between imine and enamine may be established when at least one hydrogen atom on the imine nitrogen (Scheme 1). The relative equilibrium of these species depends on the symmetry of the parent ketone and the substituents on the amine.

Since the imine bond is labile and readily hydrolyzed to the corresponding ketone, it is difficult to accurately monitor and determine which factors influence the extent of imine formation. For example, experiments using Raman and infrared spectroscopy to study the stretching frequencies of imines have been reported.[3] By studying the kinetics of imine formation from acetophenone and substituted aniline, Lee et al. were successful in monitoring the conversion from a ketone to an imine.[3] Egawa and Konaka[4] reported a study on the molecular structure of 2-butanimine, determined from gas-phase electron diffraction experiments as well as MP2 and DFT calculations. Their results indicate the (*E*)-sp con-

* Corresponding author phone: (336)334-4257; fax: (336)334-5402; e-mail: jpbowen@uncg.edu.
[†] University of North Carolina at Greensboro.
[‡] University of Georgia.
[§] University of North Carolina at Chapel Hill.

10.1021/ct049890p CCC: $30.25
Published on Web 02/15/2005

Scheme 1. Possible Reaction Pathway and Equilibria from Ketones to Enamines to Imines

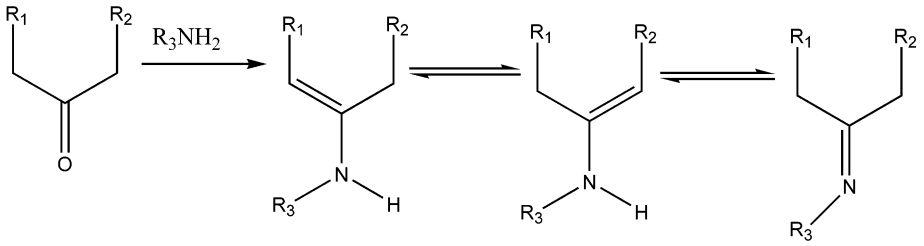

formation as the most favorable for 2-butanimine. The use of an assumed dihedral angle (φNCCC at 117.6°), however, introduces bias into the calculations. A number of additional computational studies focusing on ketones and/or imines have also been reported.[5,6] However, all of the aforementioned experimental and computational studies did not address imine-enamine tautomerism. In addition, the factors influencing the conformational preferences for the relevant ketone, imine and enamine have not been established.

Our interest in the conformational preferences of imines stems in part from ongoing investigations into understanding the structural requirements for enzyme choline acetyltransferase (ChAT) inhibitors. Effective inhibitors of ChAT presumably will reduce the levels of acetylcholine. This leads to intriguing suggestion that ChAT inhibitors, alone or coupled with other agents, might be used as potential prophylactic protecting agents for those who might be exposed to nerve gases that block acetylcholine esterase as their mechanism of action.[7] Among the types of inhibitors of ChAT reported, *trans*-*N*-methyl-4-(1-naphthylvinyl)pyridine (NVP) analogues (Figure 1)[8−10] represent the most

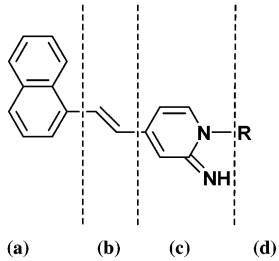

Figure 1. *trans*-1-Alkyl-4-(1-naphthylvinyl)pyridinium (NVP) analogue.

extensively explored compounds for structure activity relationship (SAR) purposes using classical approaches. NVP analogues are divided into four regions labeled ***a***, ***b***, ***c***, ***d*** (Figure 1). Region ***a*** contains an aromatic group that is attached via a *trans*-ethylene linkage, region ***b***, to a pyridinium ring that comprises region ***c***. Region ***d*** defines the various alkyl groups that can be bonded to the pyridinium nitrogen. In region **c**, 2-pyridone-imine analogues of NVP were also reported as a stronger base than pyridine.[8] Reports also show that an imine moiety −N═CH in region **b** enhances the activity.[9] All of these stimulated our interest in the fundamental conformational aspects of imines, how they differ from the corresponding carbonyl functional groups, and what significance this could have on inhibitor design.

To provide insight into imine-enamine tautomerism as well as the factors that determine the conformational preferences of ketones, imines, and enamines, we performed ab initio RHF/6-311G**, MP2/6-311G** and DFT B3LYP/6-311G** calculations on various ketones and aldehydes and their corresponding imines and enamines: i.e., 2-butanone, *Z*/*E*-2-butanimine, 1-butenamine, and *Z*/*E*-2-butenamine, propanal, *Z*/*E*-propanimine, and *Z*/*E*-propenamine (Figure 2). We also hoped to investigate the effect of the *Z*/*E* configurations of these compounds on their conformations.

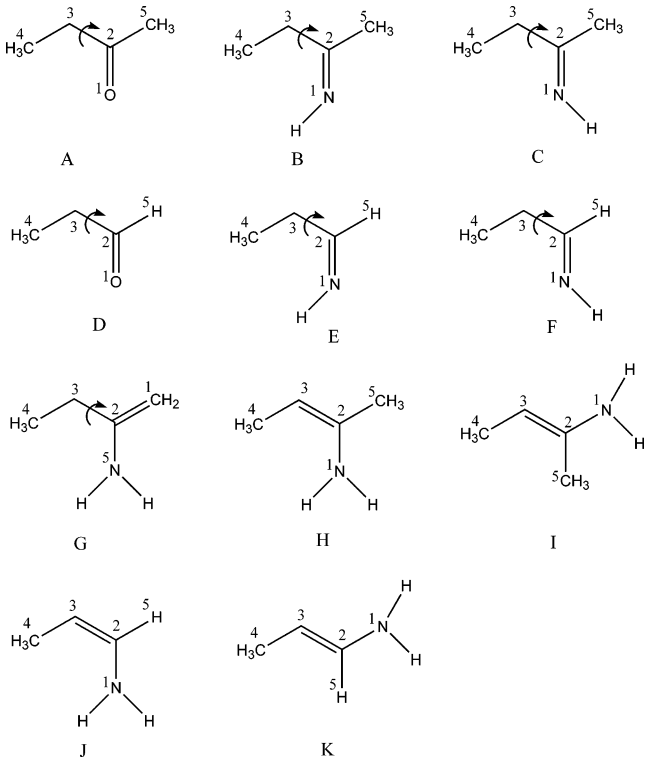

Figure 2. Chemical structures of 2-butanone (A); *Z*-2-butanimine (B); *E*-2-butanimine (C); propanal (D); *Z*-propanimine (E); *E*-propanimine (F); 1-butenamine (G); *Z*-2-butenamine (H); *E*-2-butenamine (I); *Z*-propenamine; and *E*-propenamine.

Methods

In the present study, all ab initio and density functional theory (DFT) calculations were carried out using the Gaussian03 package.[11] The RHF and the Møller−Plesset perturbation theory (MP2)[12] of ab initio methods and Becke's three parameter exact exchange functional (B3)[13] combined with gradient corrected correlation functional of Lee−Yang−Parr (LYP)[14] of the DFT method have been employed to optimize the geometry by implementing the 6-311G** basis set. During both SCF and geometry optimizations, the default convergence criteria were used. For seven molecules in

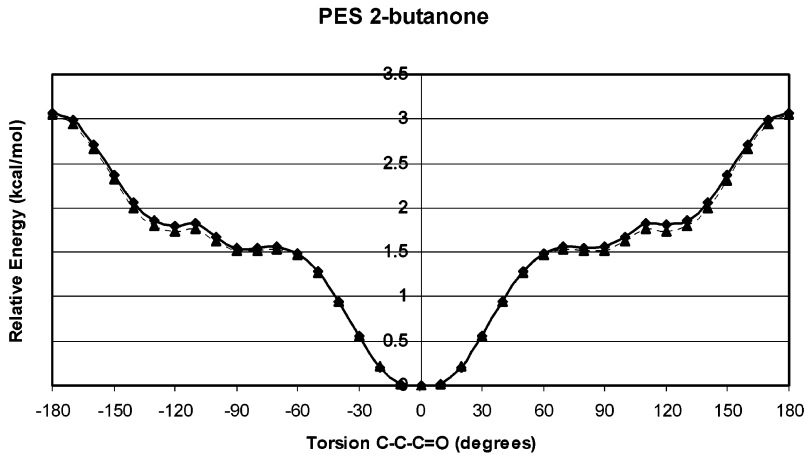

Figure 3. Potential energy surface for 2-butanone at MP2/6-311G** (diamond, black) and at RHF/6-311G** (grey, triangle).

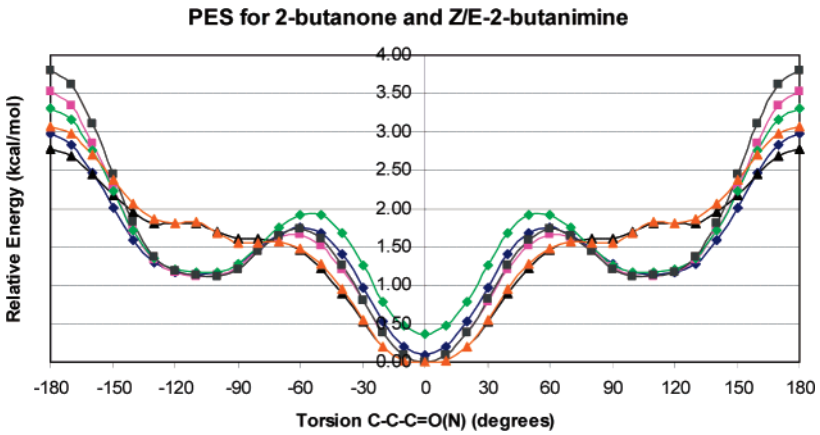

Figure 4. Potential energy surface for 2-butanone and its analogues. The color codes are *Z*-2-butanimine (B3LYP, blue, diamond); *E*-2-butanimine (B3LYP, magenta, square); 2-butanone (B3LYP, black, triangle); *Z*-2-butanimine (MP2, green, diamond); *E*-2-butanimine (MP2, gray, square); and 2-butanone (MP2, orange, triangle), respectively.

Figure 2 (A to G), complete exploration of their conformational space was carried out along the coordinate of the dihedral angle as defined by atom1-atom2-atom3-atom4 over a range of 360.0° at an increment of 10.0°. All reported minima along the potential energy surface were subjected to full geometry optimizations. The minima were confirmed using frequency calculations. The infrared data are reported, and the respective infrared peak assignments were confirmed by Gaussview. Transition structures were located using the STQN method and were confirmed with frequency calculations. For molecules H to K in Figure 2, no dihedral scan was applied because of the coplanar nature of the C═C double bonds, and only optimization and frequency calculations were carried out. NBO charges were determined for each of the optimized stationary points. Solvent effects for the minima were investigated by performing single-point energy calculations using self-consistent reaction field (SCRF) theory with the isodensity surface polarized continuum model (IPCM) method in Gaussian03 at the RHF/6-311G**.[15] The SCRF−IPCM calculations were carried out in chloroform, methanol and water at 298.15 K with solvent dielectric constants of 4.90, 32.63, and 78.39, respectively.

Results and Discussion

The PES maps for the seven molecules in Figure 2 (A to G), derived from RHF/6-311G**, MP2/6-311G**, B3LYP/6-311G** levels of theory, are given in Figures 1S-7S (see Supporting Information). As shown in Figure 3, the PES trajectories from RHF/6-311G** (grey dash line) and MP2/6-311G** (black line) are very close. To simplify the comparisons, only data from MP2/6-311G** and B3LYP/6-311G** are reported in the PES figures herein. Systematic searching of the conformational space for 2-butanone from MP2/6-311G** yielded five minima. As defined by the $C_4-C_3-C_2=O$ torsional angles, these angles were approximately 0.0°, 90.0°, 120.0°, −120.0°, −90.0° (Figure 3). The symmetry of 2-butanone provides for a conformational degeneracy in the molecule and gives rise to only three distinct conformations. There are only two distinct minima for both *Z*- and *E*-2-butanimine (Figure 4), where *Z*- and *E*- designate the configuration of the N−H bond (cis and trans to the ethyl group, respectively). The gas-phase energies and characteristic torsion angles for all seven minima are reported in Table 1. The differences in energy for these seven minima are less than 4.00 kcal/mol. In any case, the cis conformation has the lowest gas-phase energy (Table 1 and Figures 3 and 4). The cis, skew, gauche, and trans conformations as defined by the $C_4-C_3-C_2=O$ dihedral angle are 0.0°, 90.0°, 120.0°, 180.0°, respectively. The activation energy barriers among each of these three minima are less than 2.0 kcal/mol, indicating that these conformations are interchangeable at room temperature.

Table 1. Ab Initio and DFT Gas-Phase Energies and Characteristics of the Conformers for 2-Butanone and Analogs Calculated at the 6-311G** Level of Theory

conformer	name	torsion[a]	HF energy (Hartree)	ΔE (HF) (kcal/mol)	MP2 energy (Hartree)	ΔE (MP2) (kcal/mol)	B3LYP energy (Hartree)	ΔE (B3LYP) (kcal/mol)
1	*cis*-butanone	0.0	−231.058385417	0.00	−231.056291767	0.00	−232.538467751	0.00
2	*skew*-butanone	85.4	−231.055975740	1.51	−231.053829221	1.55	−232.535899977	1.61
3	*gauche*-butanone	120.8	−231.055619900	1.74	−231.053401635	1.81	−232.535608393	1.79
4	*trans*-butanone-TS	180.0	−231.053509290	3.06	−231.051406829	3.07	−232.534052150	2.77
5	*cis-Z*-butanimine	0.0	−211.206000593	0.39	−211.203861555	0.36	−212.650927530	0.09
6	*gauche-Z*-butanimine	104.1	−211.204828851	1.12	−211.202506462	1.21	−212.649273550	1.13
7	*trans-Z*-butanimine-TS	180.0	−211.201297364	3.34	−211.199159258	3.31	−212.646346026	2.97
8	*gauche-Z*-butanimine-TS	60.4	−211.203570010	1.91	−211.201379150	1.92	−212.648286182	1.75
9	*cis-E*-butanimine	0.0	−211.206615733	0.00	−211.204438625	0.00	−212.651078141	0.00
10	*gauche-E*-butanimine	101.6	−211.204920944	1.06	−211.202663787	1.11	−212.649302964	1.11
11	*trans-E*-butanimine-TS	180.0	−211.200556444	3.80	−211.198371715	3.81	−212.645467645	3.52
12	*gauche-E*-butanimine-TS	60.0	−211.203946883	1.67	−211.201683488	1.73	−212.648431749	1.66
13	2-butyl-*E*-enamine	−3.1	−211.197879766	5.48	−211.196080926	5.24	−212.646451815	2.90
14	2-butyl-*Z*-enamine	174.3	−211.195768495	6.81	−211.194132716	6.47	−212.644203418	4.31
15	1-butyl-enamine-0	177.4	−211.196500492	6.35	−211.194955066	5.95	−212.643305187	4.88
16	1-butyl-enamine-110	−71.7	−211.196617694	6.27	−211.195066736	5.88	−212.643408341	4.81
17	1-butyl-enamine-n110	64.5	−211.197357797	5.81	−211.195763110	5.44	−212.643943377	4.48

[a] Torsion angle as Φ(C4-C3-C2=O/N) (degrees).

Table 2. Comparison of Calculated and Observed Infrared Frequencies (cm^{-1}) and Vibrational Assignment for 2-Butanone from RHF/6-311G**[a]

observed infrared (gas)	calculated			assignment
	cis (0)	gauche (60)	skew (90)	
2902	3252 (2904)	3250 (2902)	3250 (2902)	CH_3 symmetric stretch
2892	3238 (2891)	3235 (2889)	3239 (2892)	CH_2 symmetric stretch
1739	1993 (1780)	1991 (1778)	1993 (1780)	C=O stretch
1360	1525 (1361)	1520 (1358)	1520 (1358)	CH_3 symmetric deformation
1186	1287 (1149)	1328 (1186)	1318 (1177)	CH_3 in-plane rock

[a] The frequency data within parentheses are scaled from the calculated data by a factor of 0.8929.

Ab initio calculations have previously been carried out for 2-butanone.[5,16,17] In previous calculations, however, full geometry optimizations failed to give three distinct conformations. By allowing the torsional coordinate to vary by 10.0° increments from 0.0° to 180.0° and constraining all other structural parameters to those obtained from the optimized trans conformation, Durig et al.[5] reported only two minima for 2-butanone, one in which the $C_4-C_3-C_2=O$ torsion angle was 0.0°, and the other at 100.0°. Wiberg and Martin[16] found that the skew conformer ($C_4-C_3-C_2=O$ at 110.0°) was 2.05 kcal/mol higher in energy than the eclipsed (cis) geometry. Our data show that the *gauche*-butanone ($C_4-C_3-C_2=O$ at 120.0°) is about 1.81 kcal/mol higher in energy than the eclipsed (cis) geometry (Table 1), which is in good agreement with Wiberg's paper. Both papers, however, reported an energetically flat region between 90.0° and 120.0°. The inability to locate a third minimum in previous studies probably results from the application of geometrical constraints or the optimization of the trans and gauche conformations without a torsional scan. Using MM2 calculations, Bowen et al. also reported an energetically flat region in the PES between 70.0° and 130.0°.[17] The nature of this region makes the minima at 90.0° and 120.0° indistinguishable. In addition, different model chemistries (basis sets) yield slightly different results. As shown in Figure 4 and Figure 1S, PES of 2-butanone from RHF is not as flat as those from MP2 and B3LYP. The PES trajectory of 2-butanone from B3LYP is so flat between 90.0° and 120.0° that the minima region seems like a shoulder region. The full optimization of the geometries at 90.0° and 120.0° gave two minima, with energies 1.61 and 1.79 kcal/mol above the cis conformer.

To our knowledge, we are the first to locate three distinct minima along the PES of 2-butanone (Figures 3 and 4). The energy difference between the minima at 90.0° and 120.0°, derived from MP2, is approximately 0.26 kcal/mol. The activation energy barrier from gauche (120.0°) to skew (90.0°) and from skew (90.0°) to cis (0.0°) is less than 0.2 kcal/mol. These minor energy differences suggest that the cis and the skew/gauche conformations are readily interconvertible. The energy difference between the cis and gauche/skew forms and the preference of the cis conformation are in very good agreement with other experimental[18] and computational results.[5,16,17] All three minima of 2-butanone were geometrically optimized and subsequently confirmed by frequency calculations. The major peaks of the calculated infrared spectra of these three minima, which were derived from the RHF/6-311G** torsional scan of 2-butanone, are listed in Table 2 and are compared with experimental data.[5] The excellent agreement between our calculated infrared frequencies and the experimental values demonstrates the calculation reliability.

Table 3. Comparison of Calculated and Observed Infrared Frequencies (cm^{-1}) and Vibrational Assignment for 2-Butanimine from RHF/6-311G**[a]

observed infrared (gas)	calculated				assignment
	Z-cis	*Z-gauche*	*E-cis*	*E-gauche*	
2894	3231 (2884)	3232 (2885)	3236 (2889)	3233 (2886)	CH_3 symmetric stretch
1652	1897 (1694)	1896 (1693)	1899 (1696)	1897 (1694)	C=N stretch
1385	1561 (1393)	1551 (1385)	1556 (1389)	1542 (1376)	CH_3 symmetric deformation
1286	1426 (1273)	1459 (1302)	1432 (1278)	1451 (1295)	CH_2 wag + CNH bend
878	966 (862)	971 (869)	952 (850)	951 (849)	C-C=N-H torsion

[a] The frequency data within parentheses are scaled from the calculated data by a factor of 0.8929.

In contrast to 2-butanone, the torsional scan of 2-butanimine from all three models resulted in two minima: a cis and gauche conformation at 0.0° and 110.0°, respectively, as defined by the $C_4-C_3-C_2=N$ dihedral (Figure 4). The energies for these minima as well as their transition states (with a "TS" tag) are listed in Table 1. Our data implies that the *Z*/*E* configuration of the C=N double bond does have an influence on the relative energy of the minima; the *E*-form (grey, square in Figure 4) is about 0.36 kcal/mol lower in energy than the *Z*-isomer (green, diamond in Figure 4). In Table 3, the calculated infrared frequencies of *Z*/*E*-butanimine derived from RHF/6-311G** are listed and compared to those from experiments.[19] The scaled calculated C=N stretching frequency at 1693 cm^{-1} and $C_3-C_2=N-H$ torsional frequency at 869 cm^{-1} are close to those observed experimentally (1652 cm^{-1} and 878 cm^{-1}, respectively). The good agreement between the calculated and observed frequencies strongly suggests the accuracy of our calculations. Table 3 also shows that the *E*-configuration has a lower C−C=N−H torsional frequency than the *Z*-configuration. This observation further confirms that the configuration of the C=N bond does influence properties of different configurations. Among the four minima of 2-butanimine, our calculations show that the *cis*-(*E*) conformation has the lowest energy. This observation agrees very well with the computational results from other groups.[4,6]

Our results show a deep energy well for 2-butanimine in the region of 90.0° to 120.0°, whereas the corresponding region for 2-butanone gives a relatively flat energy well. The activation energy barrier from the *gauche*-butanimine to the *cis*-butanimine is about 0.6−0.8 kcal/mol and is much larger than that of the *gauche*- to *skew*- and the *skew*- to *cis*-butanone (<0.2 kcal/mol). Such an energy difference contributes to a larger population of the imine gauche form and produces the deep well in the butanimine PES between 60.0° and 90.0°.

The Newman projections and natural charge populations for all minima and transition structures (with a "TS" tag) for 2-butanone and its imines are illustrated in Figures5−7. Note that the charges of the terminal methyl groups are given as the sum of the charges on the methyl carbon atom and the three attached hydrogens. As shown in Figures 5−7, the stabilizing interaction leading to a preference for eclipsing of the methyl group with the carbonyl group or imine group cannot be explained by steric interaction alone. Although it is true that such a steric interaction poses a highly unfavorable hindrance for the transition structures *trans*-butanone and *trans*-*E*/*Z*-butanimine, such a steric interaction by itself cannot explain why the *gauche*-*Z*/*E*-butanimine is an energy minimum, while *gauche*-*Z*/*E*-butanimine-TS is a transition structure due to the fact that the distance between two

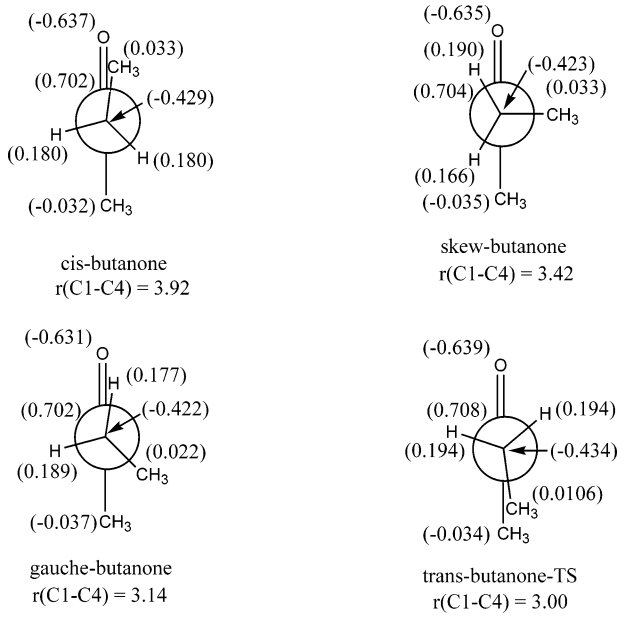

Figure 5. Newman projection structures and partial charges for atoms of 2-butanone.

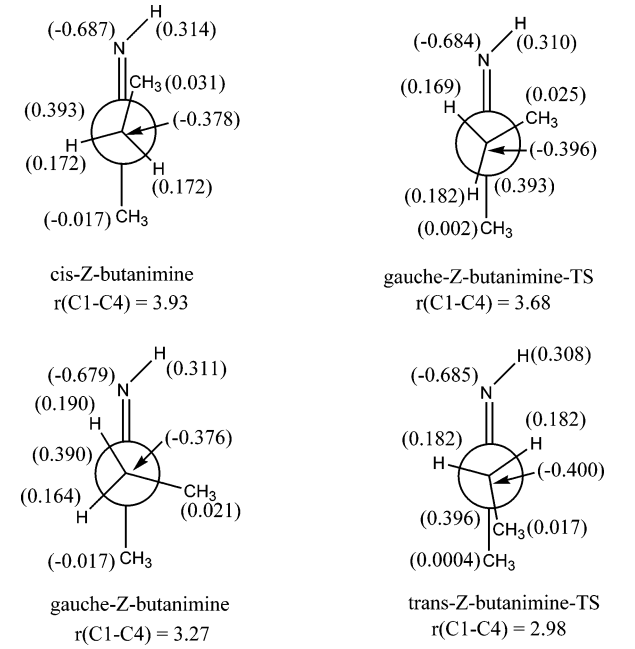

Figure 6. Newman projection structures and partial charges for atoms of *Z*-2-butanimine.

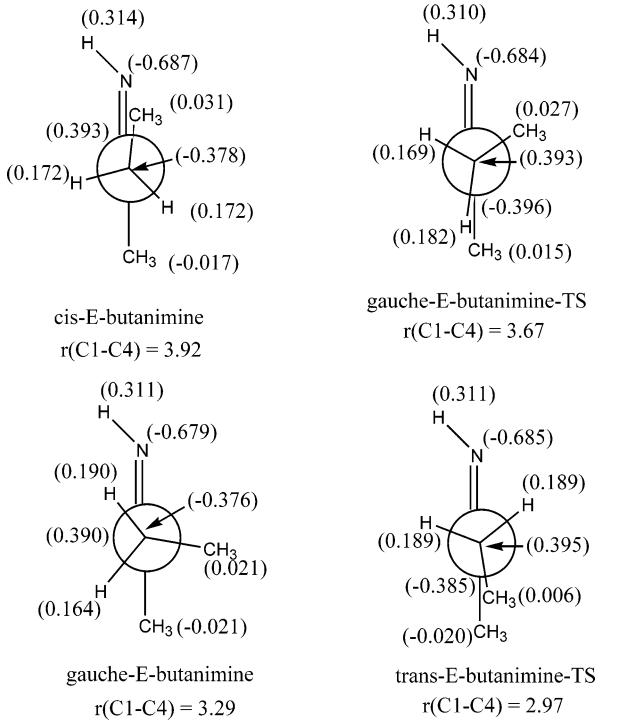

Figure 7. Newman projection structures and partial charges for atoms of *E*-2-butanimine.

terminal carbons is 3.27 Å for the former and 3.68 Å for the latter (Figure 6). However, the bond dipole interaction between the C═O and the $-CH_2-CH_3$ is maximized in *cis*-butanone because of the *anti*-parallel orientation of two bond dipoles. Though the dipole for the C═O group and the C−H bond in *gauche*-butanone is in the parallel orientation, the increasing steric interaction between two terminal methyl groups leads to a higher energy minimum for the *gauche*-butanone. Although there is an angle of roughly 20.0° between the opposite dipoles of the C═O and C−H bonds, the distance between the two terminal methyl groups in the *skew*-butanone is larger, and, thus the steric interaction is minimized. Each of these factors contributes to a minimum energetically more favorable than the *gauche*-butanone. As for the transition structure between the *gauche*- and the *skew*-butanone, the steric interaction between two terminal methyl groups should fall in the range defined by the *skew*- and the *gauche*-butanone. The angle between the bond dipoles along the C═O and $-CH_2-CH_3$ bonds of the transition structure is similar to that of both the *skew*- and *gauche*-butanone minima. The combination of such steric and bond dipole interactions contributes to a transition structure that is structurally and energetically similar to the skew and gauche conformation and thus results in a flat region in the PES.

Combinations of steric and bond dipole interactions can help rationalize the higher energy of the *trans*-*Z*/*E*-butanimine-TS, the lower energy of the *gauche*-*Z*/*E*-butanimine, and the even lower energy of the *cis*-*Z*/*E*-butanimine. Although the transition structure of the *gauche*-*Z*/*E*-butanimine-TS has less steric interactions than the *gauche*-*Z*/*E*-butanimine (Figures 6 and 7), the stabilizing bond dipole interaction between the C═N group and the C−H group is less dominant in the transition structure than in the gauche-minimum which may be attributed to the larger magnitude of the resultant bond dipole vector. More importantly, the combined charge of the terminal methyl becomes positive in the transition structure and subsequently introduces a highly destabilizing repulsion between the positively charged hydrogen atom of the imine and the positively charged methyl group. For *gauche*-*Z*/*E*-butanimine, the combined charge for the methyl group is negative and a stabilizing attraction between the negatively charged methyl group and the positively charged hydrogen atom on the imine exists. The combination of steric, bond dipole, and charge−charge interactions leads to a much higher energy for the transition structure of *gauche*-*Z*/*E*-butanimine-TS relative to the *gauche*-*Z*/*E*-butanimine. Therefore, a deep well appears in the region where the *gauche*-*Z*/*E*-butanimine conformation lies. The slight stability of the *E*- over the *Z*-configuration of butanimine, as shown in Figures 4−7, can also be explained by this bond dipole interaction. The orientation of the imine hydrogen atom in the *Z*/*E* form provides for a bond dipole that combines with the imine bond dipole resulting in a different composite dipole. This dipole then interacts with either the CH_2-CH_3 or the C−H dipoles. It is obvious that the hydrogen atom of the *E*-form C═NH is in a better position to produce a more favorable bond dipole and thus contribute to a lower energy minimum.

The steric, bond dipole, and charge−charge interactions also aid in understanding propanal and *Z*/*E*-propanimine conformations. Systematic torsional scans yield two minima (cis and gauche) for each of the three molecules from three different torsional scan methods (Figures 8 and 4S-6S). The energies for each of the minima and the transition structures are listed in Table 4. The Newman projections and the partial charges of propanal and *Z*/*E*-propanimine are shown in Figures 8S-10S. A favorable bond dipole interaction and a minimal steric interaction between the CH_2-CH_3 and the C(O)-H groups result in the cis conformation being the most favorable. Note that the gauche minimum has a favorable bond dipole interaction between the C−H and the C═O (or C═N) bonds and that the gauche transition structure has an unfavorable electrostatic repulsion resulting from two closely interacting positively charged hydrogen atoms. As a result, the gauche transition structure of all three analogues is much higher in energy than the gauche minima. As shown in Figure 8 and Table 4, the gauche transition structures in propanal and *Z*/*E*-propanimine, derived from three different model chemistries, have the highest energy relative to their cis minima, approximately 2.1−3.2 kcal/mol higher in energy. This leads to a deep well around the gauche minimum. Again, the *Z*/*E* configuration plays an important role in *Z*/*E*-propanimines. For example, the *cis*-*Z*-propanimines from all three methods are 0.8−1.2 kcal/mol higher in energy than their E counterparts. Other research groups have observed similar PES for propanal.[16,20] The optimized minima were further verified by the frequency calculations. The calculated infrared spectra for propanal and both propanimines show similar frequencies for the C═N stretch and C−C═N−H torsions and demonstrate that these calculations successfully reproduce the data from experiments.[20]

As mentioned earlier, during the interconversion of the carbonyl group of a ketone or an aldehyde to an imine, there

Table 4. Ab Initio and DFT Gas-Phase Energies and Characteristics of the Conformers for Propanal and Propanimines Calculated at the 6-311G** Level of Theory

conformer	name	torsion[a]	HF energy (Hartree)	ΔE (HF) (kcal/mol)	MP2 energy (Hartree)	ΔE (MP2) (kcal/mol)	B3LYP energy (Hartree)	ΔE (B3LYP) (kcal/mol)
1	*cis*-propanal	0.0	−192.003484947	0.00	−192.001350873	0.00	−193.202772379	0.00
2	*gauche*-propanal	125.2	−192.001564766	1.20	−191.999408387	1.22	−193.200639060	1.34
3	*gauche*-propanal-TS	70.0	−191.999847100	2.28	−191.997661366	2.32	−193.199007296	2.36
4	*trans*-propanal-TS	180.0	−192.000359676	1.96	−191.998256835	1.94	−193.199503493	2.05
5	*cis-E*-propanimine	0.0	−172.155841845	0.00	−172.153690609	0.00	−173.319150184	0.00
6	*gauche-E*-propanimine	120.0	−172.155092712	0.47	−172.152939119	0.47	−173.318146664	0.63
7	*gauche-E*-propanimine-TS	60.0	−172.152483243	2.11	−172.150229734	2.17	−173.315687045	2.17
8	*trans-E*-propanimine-TS	180.0	−172.152509425	2.09	−172.150437311	2.04	−173.315646499	2.20
9	*cis-Z*-propanimine	0.0	−172.153906329	1.21	−172.151773840	1.20	−173.317832209	0.83
10	*gauche-Z*-propanimine	121.9	−172.153743898	1.32	−172.151586161	1.32	−173.317037405	1.33
11	*gauche-Z*-propanimine-TS	60.0	−172.150811089	3.16	−172.148594804	3.20	−173.314511103	2.91
12	*trans-Z*-propanimine-TS	180.0	−172.151655370	2.63	−172.149591801	2.57	−173.315139277	2.52
13	*Z*-propyl-enamine	2.6	−172.148720083	4.47	−172.146764767	4.35	−173.316285220	1.80
14	*E*-propyl-enamine	180.0	−172.146175156	6.07	−172.144875228	5.53	-173.314324062	3.03

[a] Torsion angle as Φ(C4-C3-C2=O/N) (degrees).

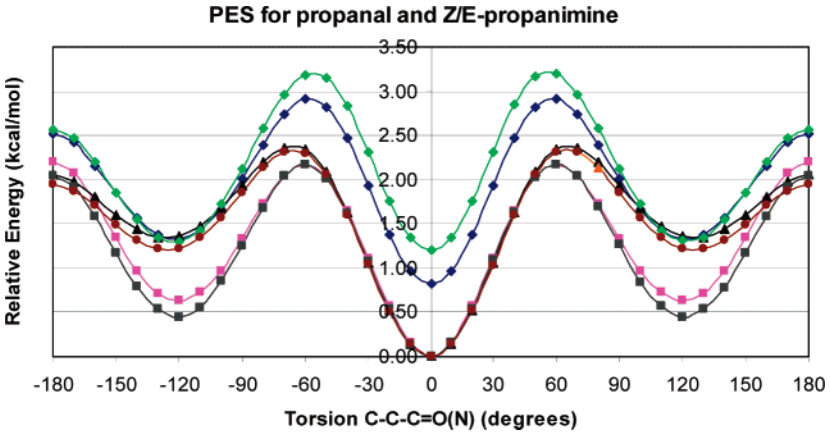

Figure 8. Potential energy surface for propanal and its analogues. The color codes are *Z*-propanimine (B3LYP, blue, diamond); *E*-propanimine (B3LYP, magenta, square); propanal (B3LYP, black, triangle); *Z*-propanimine (MP2, green, diamond); *E*-propanimine (MP2, gray, square); and propanal (MP2, orange, triangle), respectively.

exists some equilibrium between the enamine and imine structures (Scheme 1). Such an equilibrium has been reported for enaminosulfones[21] and methyl 2-acetamidoacrylates.[22] The imine-enamine tautomerism is proposed as a mechanism of the proline-catalyzed direct aldol reaction between acetone and acetaldehyde.[23] Due to the geometry of the C═C double bond, only optimizations of 2-butyl-*Z*/*E*-enamine and *Z*/*E*-propyl-enamine were carried out. The energies of the optimized geometries are listed in Tables 1 and 4, respectively. For 1-butyl-enamine, there are three minima along the PES which was discovered from a torsional scan of the C−C−C═C dihedral angle (Figures 9 and 7S). The energies for these three minima are listed in Table 1. The relative energies of the enamines were determined based on the lowest energy of the corresponding isomeric imines (*cis*-*E*-butanimine). Through this comparison, the enamines are shown to be much higher in energy than their imine isomers, 5.2−6.8 kcal/mol higher than the *cis*-*E*-butanimine isomer in both RHF and MP2 methods. This finding suggests that the conversion of 2-butanone and propanal will predominantly yield the corresponding imine instead of enamine, which is consistent with experiments.[22] Furthermore, the calculations also show that the eclipsed configuration, the *Z* form, has lower energy than the *E*-configuration (Tables 1 and 4). The energetic difference can be attributed mainly to minimal steric hindrance in the *Z*-configurations (Figure 11S, in Supporting Information). The stability of 1-butyl-enamine-n110 is likely to be the result of less steric interaction between the C═CH_2 and the terminal CH_3 groups and better bond dipole interaction between the C−CH_3 and the C−NH_2 bonds. The small energy difference between the lowest energy minima for 1-butenamine and 2-butenamine suggests that if there is any equilibrium between imines and enamines, these two butenamines may have approximately equal populations.

The solvent effect on the optimized minima was calculated using the IPCM method and is shown in Table 5. For 2-butanone and propanal, the cis conformations not skew- or gauche-conformations are still preferred in chloroform, methanol, and water. For propanimines, *cis*-*E*-propanimine has the lowest energy in the gas phase, while *gauche*-*E*-propanimine and *cis*-*Z*-propanimine are more favorable in more polar solvents, such methanol and water. Similarly, *cis*-*Z*-butanimine is more favorable in more polar solvents, while

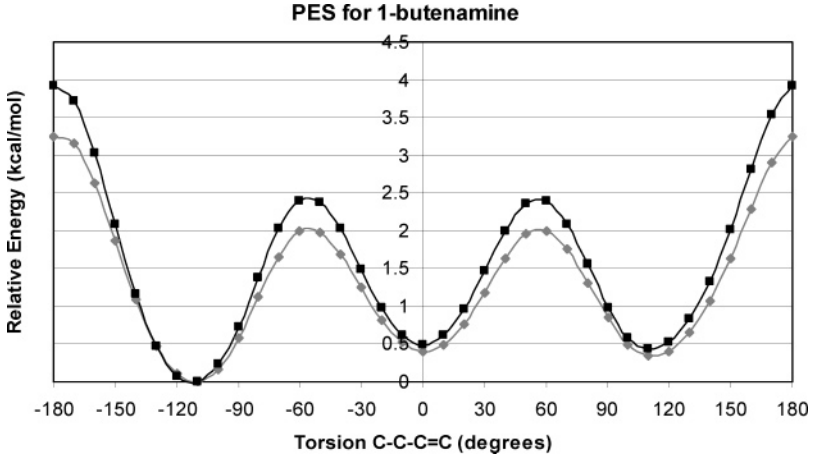

Figure 9. Potential energy surface for 1-butenamine (MP2: black square; B3LYP: gray triangle).

Table 5. Ab Initio SCRF-IPCM Energies of the Conformers for 2-Butanone, Propanal, and Their Analogs Calculated at the RHF/6-311G(2d, 2p) Level of Theory

conformer	name	torsion[a]	ΔE (gas) (kcal/mol)	energy ($CHCl_3$, Hartree)	ΔE ($CHCl_3$) (kcal/mol)	energy (MeOH, Hartree)	ΔE (MeOH) (kcal/mol)	energy (H_2O, Hartree)	ΔE (H_2O) (kcal/mol)
1	*cis*-butanone	0.0	0.00	−231.0648250	0.00	−231.0677853	0.00	−231.0681391	0.00
2	*skew*-butanone	85.4	1.51	−231.0628746	1.22	−231.0658420	1.22	−231.0661906	1.22
3	*gauche*-butanone	120.8	1.74	−231.0622612	1.61	−231.0653047	1.56	−231.0656627	1.55
4	*cis-Z*-butanimine	0.0	0.39	−211.2115951	−0.20	−211.2141008	−0.29	−211.2143951	−0.29
5	*gauche-Z*-butanimine	104.1	1.12	−211.2104819	0.50	−211.2130419	0.38	−211.2133429	0.37
6	*cis-E*-butanimine	0.0	0.00	−211.2112795	0.00	−211.2136461	0.00	−211.2139325	0.00
7	*gauche-E*-butanimine	101.6	1.06	−211.2104131	0.54	−211.2129336	0.45	−211.2132328	0.44
8	2-butyl-*E*-enamine	−3.1	5.48	−211.2010881	6.40	−211.2029120	6.74	−211.2031344	6.78
9	2-butyl-*Z*-enamine	174.3	6.81	−211.1991754	7.60	−211.2010528	7.90	−211.2012799	7.94
10	1-butyl-enamine-0	177.4	6.35	−211.2004321	6.81	−211.2024490	7.03	−211.2026928	7.05
11	1-butyl-enamine-110	−71.7	6.27	−211.2006143	6.69	−211.2026835	6.88	−211.2029344	6.90
12	1-butyl-enamine-n110	64.5	5.81	−211.2009515	6.48	−211.2029256	6.73	−211.2031691	6.75
13	*cis*-propanal	0.0	0.00	−192.0094892	0.00	−192.0122541	0.00	−192.0125835	0.00
14	*gauche*-propanal	125.2	1.20	−192.0079538	0.96	−192.0107282	0.96	−192.0110528	0.96
15	*cis-E*-propanimine	0.0	0.00	−172.1600476	0.00	−172.1622079	0.00	−172.1624707	0.00
16	*gauche-E*-propanimine	120.0	0.47	−172.1600621	−0.01	−172.1623677	−0.10	−172.1626419	−0.11
17	*cis-Z*-propanimine	0.0	1.21	−172.1597472	0.19	−172.1622479	−0.03	−172.1625386	−0.04
18	*gauche-Z*-propanimine	121.9	1.32	−172.1596196	0.27	−172.1621684	0.02	−172.1624661	0.00
19	*Z*-propyl-enamine	2.6	4.47	−172.1522905	4.87	−172.1542339	5.00	−172.1544685	5.02
20	*E*-propyl-enamine	180.0	6.07	−172.1494489	6.65	−172.1512576	6.87	−172.1514772	6.90

[a] Torsion angle as Φ(C4-C3-C2=O/N) (degrees).

cis-E-butanimine is preferred in the gas phase. The IPCM energy of each conformation of 2-butanone, propanal, and their imine analogues shows that the difference between the gas-phase energy and the IPCM energies from three different solvents decreases as the solvent polarity increases. This indicates that those conformations would be more stable in more polar solvents, e.g. methanol and/or water. For enamine, however, the energies become increasingly larger than the gas-phase energy as the solvent polarity increases. Therefore, the energy difference between enamine and the relevant imine becomes larger. Our calculations indicate that the polar solvent would stabilize the imines. These results are in very good agreement with the calculations from Rankin's paper, which reported enamine to be 27.3 kJ/mol lower than the imine in the gas phase but 9.8 kJ/mol higher than the imine in DMSO.[23]

All of our above discussions on imine linkage may help in understanding the conformational preferences for −N═CH and −CH═N moieties in NVP analogues, which might suggest a modification of the pharmacophore model.

Conclusion

Our calculations have provided an explanation for the conformational behavior of 2-butanone, propanal, and their imines and enamine derivatives. Our data suggest that for 2-butanone and propanal, steric and bond dipole interactions are primarily responsible for the conformational preferences of ketones and propanals. Additionally, charge−charge interaction might also play an important role in determining the imine conformations. In contrast, for enamines, the steric interactions are the major energy contributions, although bond dipole interactions might also exert some influence. Our results also suggest that for the conversion of butanone and/or propanal, the imine would be the predominant product, not the enamine. Lastly, our results are in good agreement with previous experimental and computational results and

should provide a better understanding of the ketone (aldehyde), imine and enamine interconversion. Moreover, the calculations strongly suggest conformational preferences in NVP analogues where the *trans*-ethylene connecting group might be replaced by imine linkages. Whether or not this has conformational implications for ChAT inhibitor design remains to be answered and will be addressed in future work.

Supporting Information Available: PES maps for the conformational scan for seven molecules in Figure 2(A to G) (Figures 1S-7S) and Newman projection structures and partial charges for atoms of propanal (Figure 8S), *Z*-propanimine (Figure 9S), *E*-propanimine (Figure 10S), and *Z*/*E*-butenamine (Figure 11S). This material is available free of charge via the Internet at http://pubs.acs.org.

References

(1) Smith, S. O.; Pardeon, T. A.; Mulder, P. P. J.; Cuny, B.; Lugtenburg, J.; Mathies, R. *Biochemistry* **1983**, *22*, 6141−6148.

(2) Vdovenko, S. I.; Gerus, I. I.; Wójcik, J. *J. Phys. Org. Chem.* **2001**, *14*, 533−542.

(3) Lee, M.; Kim, H.; Rhee, H.; Choo, J. *Bull. Korean Chem. Soc.* **2003**, *24*, 205−208.

(4) Egawa, T.; Konaka, S. *J. Phys. Chem. A* **2001**, *105*, 2085−2090.

(5) Durig, J. R.; Feng, F. S.; Wang, A.; Phan, H. V. *Can. J. Chem.* **1991**, *69*, 1827−1844.

(6) Wang, Y.; Poirier, R. A. *J. Phys. Chem. A* **1997**, *101*, 907−912.

(7) Gray, A. P.; Platz, R. D.; Henderson, T. R.; Chang, T. C. P.; Takahashi, K.; Dretchen, K. L. *J. Med. Chem.* **1988**, *31*, 807−814.

(8) Cavallito, C. J.; Yun, H. S.; Edwards, M. L.; Foldes, F. F. *J. Med. Chem.* **1971**, *14*, 130−133.

(9) Kontoyianni, M.; McGaughey, G. B.; Stewart, E. L.; Cavallito, C. J.; Bowen, J. P. *J. Med. Chem.* **1994**, *37*, 3128−3131.

(10) Chandrasekaran, V.; McGaughey G. B.; Cavallito, C. J.; Bowen, J. P. *J. Mol. Graphics Modell.* **2004**, *23*, 69−76.

(11) Frisch, M. J.; Trucks, G. W.; Schlegel, H. B.; Scuseria, G. E.; Robb, M. A.; Cheeseman, J. R.; Montgomery, J. A., Jr.; Vreven, T.; Kudin, K. N.; Burant, J. C.; Millam, J. M.; Iyengar, S. S.; Tomasi, J.; Barone, V.; Mennucci, B.; Cossi, M.; Scalmani, G.; Rega, N.; Petersson, G. A.; Nakatsuji, H.; Hada, M.; Ehara, M.; Toyota, K.; Fukuda, R.; Hasegawa, J.; Ishida, M.; Nakajima, T.; Honda, Y.; Kitao, O.; Nakai, H.; Klene, M.; Li, X.; Knox, J. E.; Hratchian, H. P.; Cross, J. B.; Adamo, C.; Jaramillo, J.; Gomperts, R.; Stratmann, R. E.; Yazyev, O.; Austin, A. J.; Cammi, R.; Pomelli, C.; Ochterski, J. W.; Ayala, P. Y.; Morokuma, K.; Voth, G. A.; Salvador, P.; Dannenberg, J. J.; Zakrzewski, V. G.; Dapprich, S.; Daniels, A. D.; Strain, M. C.; Farkas, O.; Malick, D. K.; Rabuck, A. D.; Raghavachari, K.; Foresman, J. B.; Ortiz, J. V.; Cui, Q.; Baboul, A. G.; Clifford, S.; Cioslowski, J.; Stefanov, B. B.; Liu, G.; Liashenko, A.; Piskorz, P.; Komaromi, I.; Martin, R. L.; Fox, D. J.; Keith, T.; Al-Laham, M. A.; Peng, C. Y.; Nanayakkara, A.; Challacombe, M.; Gill, P. M. W.; Johnson, B.; Chen, W.; Wong, M. W.; Gonzalez, C.; Pople, J. A. Gaussian, Inc.: Pittsburgh, PA, 2003.

(12) Mϕller, C.; Plesset, M. S. *Phys. Rev.* **1934**, *46*, 618−622.

(13) Becke, A. D. *Phys. Rev. A* **1988**, *38*, 3098−3100.

(14) Lee, C.; Wang, Y.; Parr, R. G. *Phys. Rev. B* **1988**, *37*, 785−789.

(15) Foresman, J. B.; Keith, T. A.; Wiberg, K. B.; Snoonian, J.; Frisch, M. J. *J. Phys. Chem.* **1996**, *100*, 16098−16104.

(16) Wiberg, K. B.; Martin, E. *J. Am. Soc. Chem.* **1985**, *107*, 5035−5041.

(17) Bowen, J. P.; Pathiaseril, A.; Profeta, P. S. Jr.; Allinger, N. L. *J. Org. Chem.* **1987**, *52*, 5162−5166.

(18) Abe, M.; Kuchitsu, K.; Shimanouchi, T. *J. Mol. Struct.* **1969**, *4*, 245−253.

(19) Egawa, T.; Ito, M.; Konaka, S. *J. Mol. Struct.* **2001**, *560*, 337−344.

(20) Randell, J.; Hardy, J. A.; Cox, A. P. *J. Chem. Soc., Faraday Trans. 2* **1998**, *84*, 1199−1212.

(21) Forzato, C.; Felluga, F.; Gombac, V.; Nitti, P.; Pitacco, G.; Valentin, E. *Arkivoc* **2003** (xiv), 210−224.

(22) Cativiela, C.; García, J. I.; Mayoral, J. A.; Salvatella, L. *J. Mol. Struct. (THEOCHEM)* **1996**, *368*, 57−66.

(23) Rankin, K. N.; Gauld, J. W.; Boyd R. J. *J. Phys. Chem. A* **2002**, *106*, 5155−5159.

CT049890P